

MISFIT DISLOCATION NUCLEATION SITES AND METASTABILITY ENHANCEMENT OF SELECTIVE $\text{Si}_{1-x}\text{Ge}_x/\text{Si}$ GROWN BY RAPID THERMAL CHEMICAL VAPOR DEPOSITION

C.W. LIU* J.C. STURM*, P.V. SCHWARTZ*, and E. A. FITZGERALD**

*Princeton University, Department of Electrical Engineering, Princeton, NJ 08544

**AT&T Bell Laboratories, Murray Hill, NJ 07974

ABSTRACT

A quantitative model of the effect of the selective growth on dislocation density has been developed and compared to experiments. It is concluded that the dominant dislocation nucleation source in the selective areas occurs at the specific heterogeneous sites at edges of the selective areas. This edge nucleation can be controlled by adjusting the orientation of the sidewalls.

INTRODUCTION

A critical issue in strained $\text{Si}_{1-x}\text{Ge}_x$ technology is the stability of the films to plastic relaxation. Selective growth in localized areas can not only provide the dielectric isolation for device fabrication [1], but also can increase the metastability of the strained SiGe films.

Previous studies [2], [3], have indeed qualitatively demonstrated the metastability of as-grown films by both Chemical Vapor Deposition and Molecular Beam Epitaxy in patterned oxide or on mesas. In this work, the thermal stability after post-growth annealing is investigated and a quantitative model of the metastability enhancement in selective areas is developed.

MODEL

Relaxation of strained $\text{Si}_{1-x}\text{Ge}_x$ layers occurs through the nucleation and subsequent propagation of misfit dislocations. Because of the long dislocation length, misfit dislocations can affect areas far from their original nucleation sites. The concept of selective area growth is to reduce the range over which a dislocation can propagate. Fig.1(a) shows the area over which dislocation nucleation will affect the central $W \times W$ area of interest, assuming an average dislocation length L . The number of dislocation lines N in the central $W \times W$ area is given on average by

$$N = \alpha (2LW + W^2) \quad (1)$$

where W is width of square holes and α is areal density ($\#/\text{cm}^2$) of nucleation sites.

If the same $W \times W$ area is surrounded by field oxide as in Fig. 1(b), the selective area is susceptible only to dislocations nucleated within this $W \times W$ area, but the possible nucleation from the edge of the selective areas must be taken into account. The number of dislocations in the selective area, N_s is determined by

$$N_s = \alpha W^2 + 4\beta W \quad (2)$$

where β is linear density ($\#/\text{cm}$) of nucleation sites on the edge of oxide. The ratio of N and N_s is defined as enhancement factor (EF) of the stability of the selective structure, i.e.,

$$EF = \frac{N}{N_s} = \frac{W+2L}{W+W_0} \quad , \quad W_0 = 4\beta/\alpha \quad (3)$$

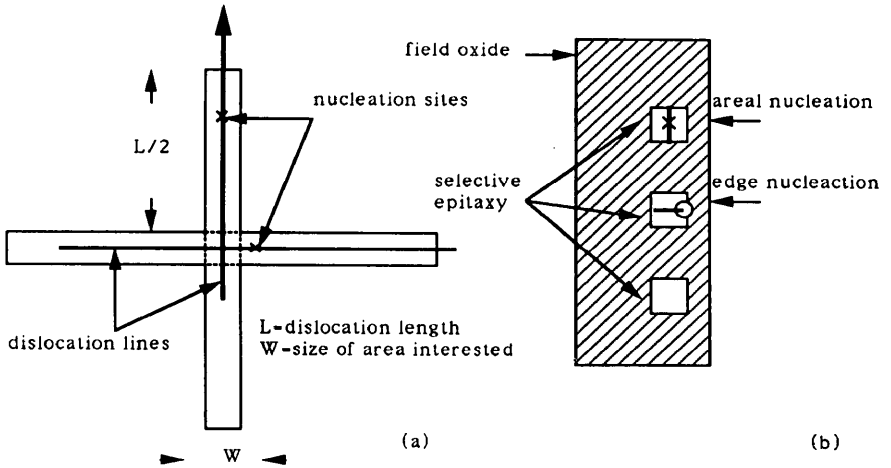


Fig. 1 Schematic diagram illustrating concept of selective growth for enhanced metastability. In non-selective growth (a), the central $W \times W$ area is susceptible to dislocations nucleated over a large cross area, which is decided by dislocation length L . In the selective growth (b), the $W \times W$ area is susceptible only to dislocations nucleated within that area, but edge nucleation must be considered.

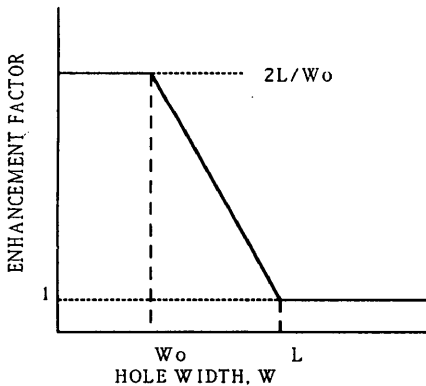


Fig. 2 A schematic curve for Enhancement Factor (EF) as a function of selective area size. For area size less than W_0 , the EF is limited by edge nucleation. For area size greater than L , there is no enhancement. Between these two extremes, the EF is inversely proportional to the hole width.

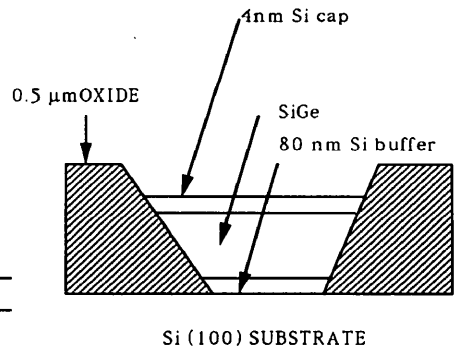


Fig. 3 The epitaxial structure of selective growth. The Si buffer and Si cap were grown at 900°C and 700°C , respectively. The SiGe was grown at 625°C .

The enhancement factor has a limiting value of unity for large W as one approaches the non-selective case. For very small W , the edge nucleation will be dominant, so that the dislocation density and enhancement factor are again independent of W . EF will then be greater or less than unity depending on the relative severity of edge nucleation compared to the dislocation length. For intermediate W , EF varies monotonically between these limiting values and is given by $2L/W$. This relationship is schematically sketched in Fig. 2, assuming $L > W_0$.

EXPERIMENTS AND DISCUSSION

To study the effect of growth area on metastability, we grew 200nm of epitaxial $\text{Si}_{.87}\text{Ge}_{.13}$ selectively in various size of square holes in thermal oxide on Si (100) wafers at 625 °C by Rapid Thermal Chemical Vapor Deposition (RTCVD) [4] (holes oriented along $\langle 110 \rangle$ directions). The structure is shown in Fig.3. After the growth, the samples were annealed at 900 °C for different periods. The dislocations were then delineated by defect etching [5], [6], with 4 parts 49% HF and 5 parts 0.3M CrO_3 , and observed under a Nomarski microscope. For reference, the thermal equilibrium critical thickness of $\text{Si}_{.87}\text{Ge}_{.13}$ is 23 nm [7].

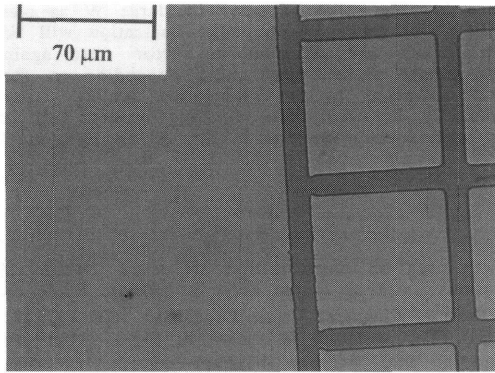
No dislocations were observed for as-grown $\text{Si}_{.87}\text{Ge}_{.13}$ layers in selective areas, and for the non-selective areas the spacing between dislocations was on the order of 1 cm. The samples with various annealing times all showed that the selective areas were more stable than the non-selective areas (Fig.4). The independence of the EF versus hole width for 5 min. annealed samples, (Fig.5, averaged over 20 samples) implies that W is less than W_0 , i.e., dislocations in the selective areas are primarily generated by edge nucleation. The low value of EF further supports the conjecture, because the EF should be around 1000 for $L=1\text{cm}$, which is the sample size, and $W=20 \mu\text{m}$ if there were no edge nucleation.

After annealing for 1 hr. and 2 hr., the dislocation lines on the non-selective areas are too close to count reliably. But X-ray diffraction shows no visible shift of strained $\text{Si}_{.87}\text{Ge}_{.13}$ peak (to within $\Delta 2\theta = 0.03^\circ$). Because the difference between strained (400) $\text{CuK}\alpha$ peak and relaxed (400) $\text{CuK}\alpha$ peak of $\text{Si}_{.87}\text{Ge}_{.13}$ is about 0.3° , the relaxation of these films is less than 10%, indicating an average spacing of dislocation lines more than $0.4 \mu\text{m}$ (the average spacing of fully relaxed layers is about 40 nm). Combined with a dislocation spacing in the selective areas of $8 \mu\text{m}$ or so, this implies an EF less than 20, consistent with previous argument.

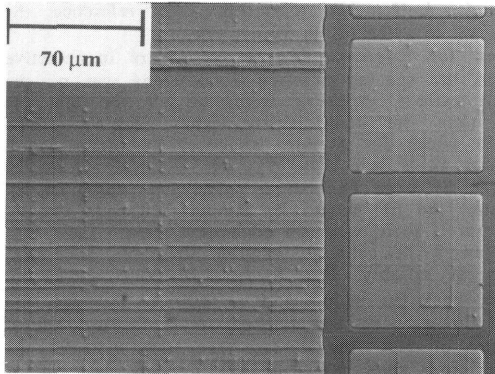
To further confirm the edge nucleation mechanism, we plot the number of dislocations versus hole width in Fig.6 for these three samples. According to e.q. (2), the linear dependence of the number of nucleation sites versus hole width indeed indicates that edge nucleation is dominant over areal nucleation. Further evidence in support of edge nucleation is that the dislocation patterns on selective areas always show that at least one end of dislocation lines terminates on oxide edges.

In Fig. 6, one can see that the number of nucleation sites hardly increases from 5 min. to 120 min. of annealing. The number of homogeneous nucleation sites should linearly increase with time, because of similar activation energy of these films in this small relaxation region (within 10%) [8]. Therefore, we conclude that the edge nucleation sites occur at some specific heterogeneous sites, possibly associated with structure defects at the oxide sidewall-epi interface.

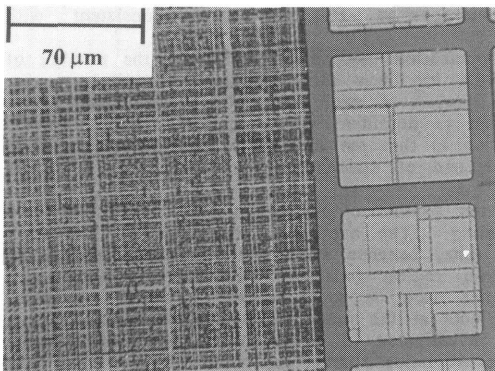
Edge nucleation was further investigated in a set of samples with 150-nm thick selective $\text{Si}_{.8}\text{Ge}_{.2}$ grown in oxide holes aligned in $\langle 110 \rangle$ direction and with 200-nm thick selective $\text{Si}_{.8}\text{Ge}_{.2}$ grown in oxide holes aligned in $\langle 100 \rangle$ direction. The $\langle 110 \rangle$ -aligned structure had a high defect density as grown in both selective and non-selective areas (Fig. 7(a)). In the $\langle 100 \rangle$ aligned samples, however, the defect density in the selective areas was markedly reduced (Fig.7(b)), despite the greater SiGe thickness. This implies a lower heterogeneous nucleation site density



(a) as-grown



(b) after 5 min. annealing



(c) after 1 hr. annealing

Fig. 4 The misfit dislocation networks of $\text{Si}_{0.87}\text{Ge}_{0.13}$ films of the thickness 200 nm annealed at 900 °C of various periods with $\langle 110 \rangle$ sidewall orientation to demonstrate the metastability enhancement of selective areas.

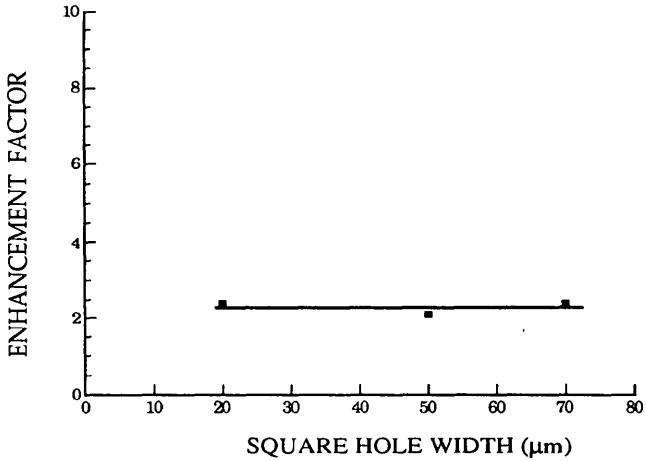


Fig. 5 Enhancement factor as a function of square width for $\text{Si}_{0.87}\text{Ge}_{0.13}$ after 5 min. annealing at 900 °C. The constant EF indicates W is less than W_0 , i.e., edge nucleation is dominant.

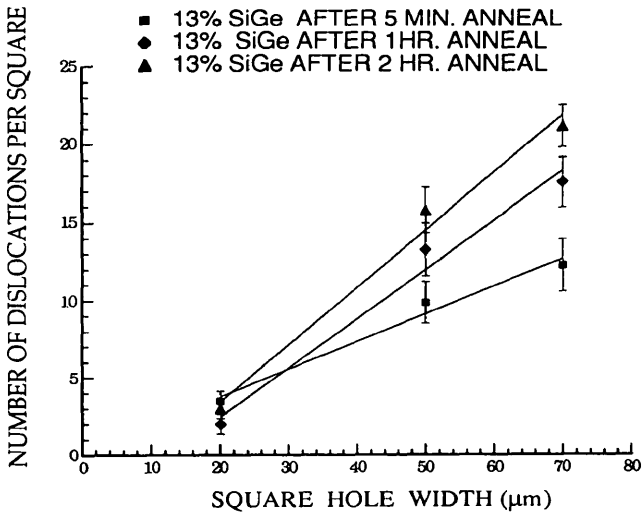


Fig. 6 The number of dislocations in selective areas as a linear function of square width for 200 nm $\text{Si}_{0.87}\text{Ge}_{0.13}$ with various annealing times at 900 °C.

(and hence defect density) along $\langle 100 \rangle$ -aligned sidewalls. Lower defect densities are indeed commonly observed in selective homoepitaxial silicon layers with the hole edges oriented in the $\langle 100 \rangle$ direction [9]. This supports the hypothesis that the edge nucleation sites are related to some defects at oxide sidewalls.

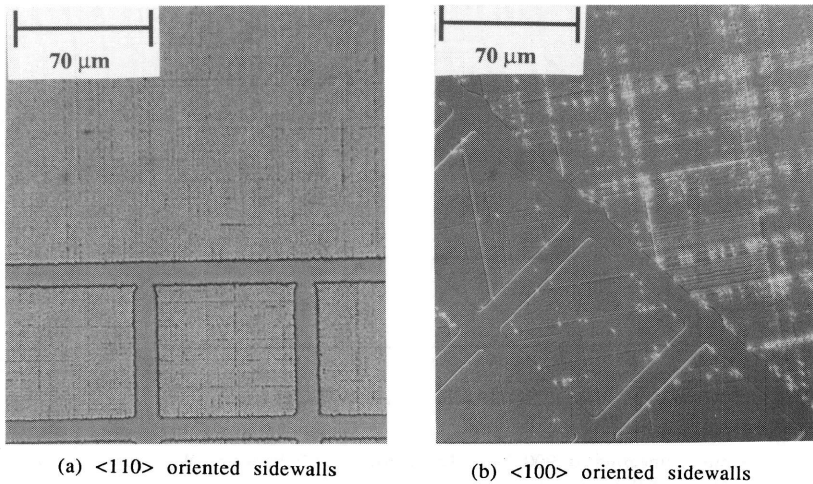


Fig. 7 The misfit dislocation networks of $\text{Si}_{0.8}\text{Ge}_{0.2}$ films with different sidewall orientation. (a) is a 150 nm film with $\langle 110 \rangle$ sidewall orientation. The defect density in selective areas is similar to that in non-selective areas. (b) is a 200 nm film with $\langle 100 \rangle$ sidewall orientation. The selective areas have lower defect densities than non-selective areas.

SUMMARY

A simple model of metastability enhancement for selective $\text{Si}_{1-x}\text{Ge}_x$ growth has been proposed. From this model, it is found that heterogeneous nucleation at the oxide edge is the dominant source of relaxation in the selective areas. The heterogeneous edge nucleation can be controlled by the sidewall orientation of the oxide holes.

REFERENCES

1. H. Hirayama, M. Hiroi, K. Koyama, and T. Tatsumi, *Appl. Phys. Lett.* **56**, 2645 (1990).
2. D. B. Noble, J. L. Hoyt, C.A. King, J.F. Gibbons, T.I. Kamins, and M.P. Scott, *Appl. Phys. Lett.* **56**, 51 (1990).
3. E. A. Fitzgerald, Y.-H. Xie, D. Brasen, M.L. Green, J. Michel, P. E. Freeland, and B.E. Weir, *J. Electronic Material*, **19**, 949 (1990).
4. J.C. Sturm, P.V. Schwartz, E. J. Prinz, and H. Manoharan, *J. Vac. Sci. Tech.* **B9**, 2011 (1991).
5. D.G. Schimmel, *J. Electrochem. Soc.*, **123**, 740 (1976).
6. C.G. Tuppen, C.J. Gibbing, and M. Hockley, *J. Cryst. Growth* **94**, 392 (1989).
7. D.C. Houghton, D.D. Perovic, J.-M. Baribeau, and G.C. Weatherly, *J. Appl. Phys.* **67**, 1850 (1990).
8. E.A. Fitzgerald, G.P. Watson, R.E. Proano, D.G. Ast, P.D. Kirchner, G.D. Pettit, and J. M. Woodall, *J. Appl. Phys.* **65**, 2220 (1989).
9. C.I. Drowley, G.A. Reid, and R. Hull, *Appl. Phys. Lett.* **52**, 546 (1988).